The role of intrinsic muscle mechanics in the neuromuscular control of stable running in the guinea fowl

Title:
The role of intrinsic muscle mechanics in the neuromuscular control of stable running in the guinea fowl.

Short title:
Neuromuscular control of stable running.

Authors: Monica A. Daley[1]*, Alexandra Voloshina[2], Andrew A. Biewener[3]

Keywords: locomotion, reflexes, preflexes, muscle function, gait, biomechanics, stability, bipedal, guinea fowl, *Numida meleagris*

*** Author for correspondence at current address:**
[1]Structure and Motion Laboratory
Royal Veterinary College, University of London
Hawkshead Lane, Hatfield, Hertfordshire
AL9 7TA
UK

[2] Human Neuromechanics Laboratory
University of Michigan
401 Washtenaw Ave
Ann Arbor MI 48109
USA

[3]Concord Field Station
Harvard University
100 Old Causeway Rd
Bedford, MA 01703
USA

Abstract:

Here we investigate the interplay between intrinsic mechanical and neural factors in muscle contractile performance during running, which has been less studied than during walking. We report *in vivo* recordings of the gastrocnemius muscle of the guinea fowl (*Numida meleagris)*, during the response and recovery from an unexpected drop in terrain. Previous studies on leg and joint mechanics following this perturbation suggested that distal leg extensor muscles play a key role in stabilisation. Here, we test this through direct recordings of gastrocnemius fascicle length (using sonomicrometry), muscle-tendon force (using buckle transducers), and activity (using indwelling EMG). Muscle recordings were analysed from the stride just before to the 2nd stride following the perturbation. The gastrocnemius exhibits altered force and work output in the perturbed and 1st recovery strides. Muscle work correlates strongly with leg posture at the time of ground contact. When the leg is more extended in the drop step, net gastrocnemius work decreases (-5.2 Jkg-1 *versus* control), and when the leg is more flexed in the step back up, it increases (+9.8 Jkg-1 *versus* control). The muscle's work output is inherently stabilising because it pushes the body back toward its pre-perturbation (level running) speed and leg posture. Gastrocnemius length and force return to level running means by the 2nd stride following the perturbation. EMG intensity differs significantly from level running only in the 1st recovery stride following the perturbation, not within the perturbed stride. The findings suggest that intrinsic mechanical factors contribute substantially to the initial changes in muscle force and work. The statistical results suggest that a history-dependent effect, shortening deactivation, may be an important factor in the intrinsic mechanical changes, in addition to instantaneous force-velocity and force-length effects. This finding suggests the potential need to incorporate history-dependent muscle properties into neuromechanical simulations of running, particularly if high muscle strains are involved and stability characteristics are important. Future work should test whether a Hill or modified Hill type model provides adequate prediction in such conditions. Interpreted in light of previous studies on walking, the findings support the concept of speed-dependent roles of reflex feedback.

Abbreviations:

C , control trials, level running; U, unexpected drop trials; LG, lateral gastrocnemius muscle; G, gastrocnemius (all heads); SONO, sonomicrometry; EMG, electromyography; L_{Ft50}, fascicle strain at 50% stance peak force; $L_{pkF,}$ fascicle strain at peak stance phase force; ΔL_{prior}, change in fascicle strain from force onset to the start of stance; V_{Ft50}, mean fascicle velocity between TD and 50% stance peak force; V_{pkF} , fascicle velocity at peak stance phase force; W_{prior}, net work before stance (2nd half of the swing phase); W_{stance}, net work during stance; W_{tot} , net work during the stride; $F_{pk,\ prior}$, peak force before stance (2nd half of the swing phase); $F_{pk,\ stance}$, peak force during stance; E_{prior} , total EMG intensity before stance; E_{stance}, total EMG intensity during stance; E_{tot}, total EMG intensity during the stride; v, running speed in meters per second; h, standing hip height; $\boldsymbol{g}$, gravitational acceleration; $\hat{u}$, dimensionless speed ($\hat{u} = v/(\boldsymbol{g}h)^{\wedge 0.5}$)

Introduction:

Runners must maintain stability when faced with sudden disturbances, such as bumps, drops and obstacles in the terrain. The mechanics and neuromuscular coordination of stable running in rough terrain is still poorly understood, but of increasing focus in the biomechanics community (Jindrich & Full, 2002; Biewener & Daley, 2007; Sponberg & Full, 2008). Most locomotion research has focused on movement over uniform surfaces (Biewener & Roberts, 2000; Dickinson *et al.*, 2000), or on perturbation recovery in slower gaits such as walking (Gorassini *et al.*, 1994; Marigold & Patla, 2005). Yet many locomotor tasks, such as predator-prey interactions, require rapid negotiation of complex terrain.

Coordination of stable movement requires integration of mechanics and neural control. A perturbation usually leads to sudden changes in musculoskeletal dynamics. These intrinsic mechanical changes can occur at many levels of the system hierarchy, including whole body velocity and potential energy, leg posture and gearing, and strain-dependent muscle tissue contractile performance (Nichols & Houk, 1973; Patla & Prentice, 1995; Brown & Loeb, 2000; Jindrich & Full, 2002; Moritz & Farley, 2004; Daley & Biewener, 2006). Since transmission and excitation-contraction coupling (ECC) delays require that muscles are activated in anticipation of action, such perturbations alter the mechanical environment in which the muscle contracts. Consequently, intrinsic mechanical changes modify the mapping between neural signal and mechanical output. Appropriate integration of musculoskeletal structure and feedforward activation of muscles may allow relatively simple intrinsic mechanical responses to stabilise locomotion, minimising the need for a rapid reflex response (Kubow & Full, 1999; Brown & Loeb, 2000; Daley & Biewener, 2006; Sponberg & Full, 2008). Nonetheless, appropriate integration with neural pathways is also important— altered mechanics leads to altered sensory feedback, and subsequent reflex mediated changes in motor output (Dietz et al., 1987; Nichols, 1994; Pearson et al., 1998). Informative models of locomotor function require a better understanding of the interplay between these mechanical and neural processes (Pearson et al., 2006; Nishikawa et al., 2007).

The relative contribution of intrinsic and neural mechanisms to movement control likely depends on speed. Less is known about the neural control mechanisms of rapid locomotion, because walking is the most often studied gait. Perturbation studies of walking cats and humans suggest that proprioceptive feedback and higher brain centres contribute to corrective stabilising responses (Dietz *et al.*, 1987; Gorassini *et al.*, 1994; Hiebert *et al.*, 1994; Hiebert & Pearson, 1999; Marigold

& Patla, 2005). However the corrective responses involve latencies of 30-200 ms. Reflex latencies require that the first 30 ms or so of stance phase extensor activity is generated centrally in a feedforward manner, because it cannot be altered by feedback (Gorassini *et al.*, 1994; Marigold & Patla, 2005). The delays associated with reflexes may cause them to be destabilising at high speeds. Consequently, it has been suggested that reflex gains tend to be reduced with increasing speed of locomotion (Capaday & Stein, 1987). Others have failed to find this trend, but noted that the reflex threshold differs between walking and running, so that reflexes contribute less to muscle activity in running (Ferris et al., 2001). Overall, these findings suggest that sensorimotor reflexes and higher brain centres likely play a larger role in slow locomotion, such as walking, whereas intrinsic mechanical factors likely play a larger role in the control of rapid locomotion, such as running.

A particularly prominent gap in current neuromechanical models of locomotion is that we know little about how intrinsic muscle properties contribute *in vivo* to control. As the only actuators and important sensors in animal neuromechanical systems, muscles form a critical link in the interplay of mechanics and control. *In vitro* and *in situ* experiments have revealed that the force and work capacity of muscle tissue depends on its strain (length), strain rate (velocity) and recent strain history (Josephson, 1993, 1999; Marsh, 1999). However, we have a limited understanding of the range of active strains normally used by muscles *in vivo*, especially during rapid and unsteady locomotor tasks (Biewener & Daley, 2007). Our knowledge of *in vivo* muscle function is based largely on measures during steady movement on a uniform surface (Biewener & Roberts, 2000; Biewener & Daley, 2007). The range of force-length dynamics of muscle during unsteady locomotion is likely to be broader than suggested by these studies.

The purpose of this study is to reveal how *in vivo* muscle force-length dynamics relate to leg mechanics and neural control of running. We investigate the stabilising response to a sudden, unexpected drop in terrain during high speed bipedal running in guinea fowl (*Numida meleagris*). This perturbation is similar in nature to previous studies on walking cats, described above (Gorassini *et al.*, 1994; Hiebert *et al.*, 1994; Hiebert & Pearson, 1999). Since only one leg is in stance at a time in bipedal running, however, the response may be more constrained than during bipedal walking or quadrupedal gaits. In previous studies of external body and leg dynamics, we found that this perturbation alters leg dynamics and loading in a stereotypic manner (Daley & Biewener, 2006; Daley *et al.*, 2006; Daley *et al.*, 2007). When the foot fails to contact the ground at the anticipated point, the hip and ankle rapidly extend until the leg reaches the true ground level

below (Daley et al., 2007). Extension at these joints results in a steeper (more vertical) leg contact angle and reduced leg loading (lower ground reaction forces) (Daley & Biewener, 2006). Additionally, the distal joints (ankle and tarso-metatarso-phalangeal), shift from spring-like to energy absorbing function when the leg is relatively extended during ground contact (Daley et al., 2007). These findings suggest that the distal hindlimb extensor muscles play an important stabilising role by rapidly altering work output depending on leg posture and leg loading.

In the current study, we focus on one particular distal hindlimb extensor muscle, the gastrocnemius (G). This muscle is extensively studied because it is experimentally accessible, and exhibits broadly similar function across many animals (Prilutsky *et al.*, 1996; Roberts *et al.*, 1997; Biewener *et al.*, 1998; Biewener & Corning, 2001; Daley & Biewener, 2003; Lichtwark & Wilson, 2006). In steady, level locomotion, the gastrocnemius muscle is activated just before stance, rapidly develops high force as the leg is loaded, and shortens with low velocity through stance to produce net positive work. Low-velocity contraction allows each muscle fibre to develop near maximal force, minimising the total volume of active muscle and the metabolic energy required to support body weight (Roberts et al., 1997; Roberts et al., 1998). The architecture of this muscle, with a pennate fibre arrangement and long tendon, facilitates economic contraction by allowing most of the muscle-tendon length change to occur in the tendinous tissues, cycling elastic strain energy (Roberts *et al.*, 1997; Lichtwark & Wilson, 2006). Consequently, it is generally thought that this muscle's primary functions are to provide economic body weight support and forward propulsion for steady locomotion, although the relative importance of each these two functions is a subject of debate (McGowan *et al.*, 2008), and may vary with species.

Recent studies have revealed that this muscle is likely capable of a broader range of mechanical roles in locomotion than previously thought. In turkeys and guinea fowl, the gastrocnemius switches between economic contraction for level running to mechanical work production for incline running (Roberts *et al.*, 1997; Daley & Biewener, 2003). New insights from 3D models of muscle also reveal that pennate muscle architecture allows variable gearing at the muscle fibre level, which could result in intrinsic switching among mechanical roles depending on loading conditions (Azizi et al., 2008). Thus, the gastrocnemius muscle is likely capable of rapidly switching between economic force development and high work output, depending on the conditions.

Here we test two hypotheses about *in vivo* function of the gastrocnemius during the unexpected drop perturbation. **1**) In the stance phase following the perturbation, gastrocnemius muscle force and work output will be reduced in association with the more extended, retracted leg posture and the reduced leg loading (Daley & Biewener, 2006; Biewener & Daley, 2007). **2**) Most of the change in muscle force and work in the stance phase immediately following the perturbation relates statistically to intrinsic mechanical factors, rather than neurally mediated changes in muscle activation.

Methods:

Animals and training:

Six female adult guinea fowl (*Numida meleagris*), 1.70±0.28 kg body mass (mean ±s.e.m., N=6), were obtained from a local breeder. Animals were housed and experiments undertaken at the Concord Field Station of Harvard University, in Bedford MA. All experimental procedures were approved and overseen by the Harvard Institutional Animal Care and Use Committee, in accordance with the regulations of the United States Department of Agriculture.

We clipped the bird's primary feathers to prevent them from flying. To ensure general fitness, we trained the birds at least 3-4 days per week for 3 weeks. During training, the birds ran for 20-30 minutes per session and were never exercised to exhaustion. On alternate days they either 1) ran at 1.7-2.0 ms^{-1} on a level motorised treadmill (Woodway, Waukesha, WI) with short breaks for 1-3 minutes every 5-10 minutes as needed and 2) ran back and forth across a level runway (0.4 m x 8 m) with short breaks as needed. Following training, the birds were able to run repeatedly across the runway at a consistent steady speed.

Muscle measurements and surgical procedures

The muscle measurements and surgical procedures were similar to those described previously (Biewener & Corning, 2001; Daley & Biewener, 2003; McGowan *et al.*, 2006). Muscle activity and fascicle strain were recorded in the lateral head of the gastrocnemius (LG) by electromyography (EMG) and sonomicrometry (SONO). We also measured muscle-tendon force of the common gastrocnemius tendon (Achilles) using a tendon buckle force transducer.

The birds were anesthetised for sterile surgery using isoflurane delivered through a mask (induction at 3-4%, maintained at 1–2.5%). The surgical field was plucked of feathers and sterilised with

antiseptic solution (Prepodyne, West Argo, Kansas City, MO). The transducers were passed subcutaneously from a 1–2 cm dorsal incision over the synsacrum to a second 4–5 cm incision over the lateral side of the right shank. An E-type stainless steel tendon buckle force transducer was implanted on the Achilles tendon. SONO crystals (1.0 mm, Sonometrics Inc., London, Canada) were implanted through small openings made with fine forceps. Crystals were placed approximately 3–4 mm deep and 10 mm apart along the fascicle axis in the middle 1/3rd of the muscle belly. Crystals were secured with 5-0 silk suture after verification of signal quality with an oscilloscope. Fine-wire, twisted, silver bipolar EMG hook electrodes (0.1 mm diameter, 0.5 mm bared tips, 5-8 mm spacing, California Fine Wire, Inc., Grover Beach, USA) were implanted immediately adjacent to the pair of SONO crystals using a 23 gauge hypodermic needle and secured to the muscle's fascia using 5-0 silk suture. Skin incisions were closed using 3-0 silk. All birds were ambulatory within 2 hours post surgery and ran the following day without apparent lameness. Experimental recordings took place over the next 1-2 days. Throughout the post-surgery experiments, the birds were given analgesia every 12 hours and antibiotics every 24 hrs. Upon completion of experimental recordings, the guinea fowl were killed by an intravenous injection of sodium pentobarbital (100 mg kg^{-1}), while under deep isoflurane anaesthesia (4%, mask delivery).

The tendon force buckles were then calibrated *in situ* post mortem as described previously (Daley & Biewener, 2003). Before buckle calibration, we dissected each muscle free from the surrounding tissues to confirm placement of tendon buckles, SONO crystals and EMG electrodes, and make morphological measurements of the muscle. Crystal alignment relative to the fascicle axis (α) was within ± 2°, indicating that errors due to misalignment were < 1%. Morphological measures of the whole gastrocnemius (G_{tot}) and lateral head (LG) were as follows (mean ± s.e.m., N=6): wet muscle mass (G_{tot}: 23 ± 3.8 g, LG: 9.1 ± 1.5 g), mean fascicle length (LG: 17.8 ± 0.5 mm), pennation angle (LG: 23 ± 2°), physiological cross-sectional area of the muscle (G_{tot}: 1134 ± 190 mm^2, LG: 445 ± 75 mm^2), and the cross-sectional area of the common 'Achilles' tendon (G_{tot},: 8.5 ± 1.2 mm^2).

Data Recording and kinematics

The transducer leads were connected *via* a micro-connector on the bird's back (GM-6, Microtech Inc, Boothwyn, PA USA) to a lightweight 10 m shielded cable (Cooner Wire, Chatsworth, USA). The cable passed to a pulley system on the ceiling to allow low-friction sliding of the cable as the bird ran across the runway. The pulley system was adjusted ensure that it did not tug on the bird at

any point in the trials. The cable connected at the other end to a sonomicrometry amplifier (120.2 , Triton Technology Inc., San Diego, USA), a strain gauge bridge amplifier (2120, Vishay Micromeasurements, Raleigh, USA), and EMG amplifiers (P-511, Grass, West Warwick, USA). EMG signals were amplified 1000X and filtered (10 Hz – 10 kHz bandpass) before digital sampling. The outputs of these amplifiers were sampled by an A/D converter (Axon Instruments, Union City, USA) at 5 kHz and stored on a computer.

Digital high-speed video was recorded in lateral view at 250 frames per second (Photron Fastcam-X 1280 PCI; Photron USA Inc., San Diego, CA, USA). This imaged the middle 1.8 m section of the runway, which was constructed of 6 mm Plexiglas™, resulting in kinematic data for approximately 3 strides. A post-triggered voltage pulse stopped the video recording and synchronised the video sequence to the muscle recordings. Kinematic points were marked on the synsacrum, hip and middle toe, and tracked using custom software in MATLAB (v7, Mathworks, Inc.; Natick, MA, USA). We noted the following kinematic time points: 1) midswing (MS), the time at which the swing-leg toe crossed the midline of the stance leg; 2) toe down (TD), when the middle toe contacted the substrate; and 3) toe off (TO), when the middle toe left the substrate. In perturbation trials, we also noted the time at which the foot first contacted the tissue paper. From these data, we calculated running speed, stride duration, stance duration, duty factor, effective leg length, leg angle, and hip height. Consecutive MS time-points were used to cut the data into stride cycle segments for analysis and averaging.

Experimental protocol

We used an unexpected drop perturbation procedure in which the birds encounter a tissue-paper camouflaged drop in terrain height. This protocol has been used in previous studies on body and leg mechanics (Daley & Biewener, 2006; Daley *et al.*, 2006; Daley *et al.*, 2007). More detailed descriptions, images and videos of the perturbation experiment are available in the previous publications. In 'Unexpected Drop' trials (U), the bird encountered a drop in terrain at the midpoint of the runway. The terrain drop was 0.6 m long (approximately one stride length), and hidden by white tissue paper pulled tightly across the gap. This created the appearance of a continuous level white runway. In training and 'Control' trials (C), the bird ran steadily across a level runway with the same appearance, in this case with a board under the white tissue paper section. U trials were limited to 2-3 trials per recording day, randomised among 15-20 C trials to minimise potential

learning effects. In a previous study we found no evidence of learning over the course of the experiment when using this randomised protocol (Daley et al., 2006).

Data processing and analysis of muscle performance

For U trials, we processed the data only if the recording (right) leg encountered the perturbation. This resulted in a sample size of 2-3 U trials per individual. We also processed 3 C trials for each individual, choosing the trials that were closest to the average running speed of the U trials. We analysed the following stride sequence (Fig. 1): the stride prior to (Stride -1), the stride on (Stride 0), the first stride following (Stride +1), and the second stride following (Stride +2) the drop section. The birds began to decelerate at around Stride +4 in anticipation of the end of the runway. In C trials, the same sequence of strides was analysed (Strides -1 to +2), providing a total of 12 control level strides per individual. Reference level stride cycle traces were calculated for each individual by calculating the mean and 95% confidence interval of all 12 C strides (Fig. 2). However we included only C Stride 0 in the ANOVA, to maintain a balanced data set.

We calculated the myoelectric intensity of the EMG signal in time-frequency space using wavelet techniques (von Tscharner, 2000; Wakeling et al., 2002). We used a bank of 16 wavelets with time and frequency resolution optimised for muscle, with wavelet centre frequencies ranging from 6.9 to 804.2 Hz (von Tscharner, 2000). From this wavelet decomposition, we summed the intensity over wavelets 2-16 at each time-point to calculate the instantaneous myoelectric intensity (mV^2). This provides a smooth trace of EMG intensity over time that accounts for the entire physiological frequency range and effectively excludes motion artefact noise from the calculation. Total EMG intensity over a given time period (E_{tot}) was calculated by integrating this myoelectric intensity over time (mV^2s).

Sonomicrometry analysis followed methods described previously (Biewener & Corning, 2001; Daley & Biewener, 2003). Raw sonomicrometry data were filtered using a smoothing cubic spline in Matlab ('spaps', tolerance = 0.0001, spline toolbox). Instantaneous muscle fascicle strain (unitless length, L) was calculated by dividing the length measured between the crystals (L_{seg}) by the resting length (L_{st}), measured while the animal stood still at rest ($L = L_{seg}/L_{st}$). It is important to note that this resting length, $L_{st,}$ is not the same as the optimal length for isometric force development, which was not measured here. As a convention, shortening strains are negative, and lengthening strains are positive.

Changes in instantaneous LG fascicle strain were differentiated with respect to time to obtain muscle fascicle velocity (in lengths per second, Ls^{-1}). For calculations of muscle work, strain and velocity were converted to absolute units (meters and ms^{-1}) by multiplying by the mean anatomical fascicle length of the muscle. LG fascicle velocity (ms^{-1}) was multiplied by instantaneous Achilles tendon force to estimate muscle power for the entire gastrocnemius group (G), assuming all heads undergo similar strains as measured in the lateral head (Daley & Biewener, 2003; Gabaldon *et al.*, 2004). Muscle power was integrated over time for each stride to provide a cumulative measure of work, in which the final value is the net muscle work per stride (in Joules). This value was divided by total gastrocnemius muscle mass to provide mass-specific work (Jkg^{-1}).

We measured a number of variables to test for differences in muscle force, strain and activation among stride categories. Potential intrinsic factors in muscle contractile performance include instantaneous strain (length), instantaneous strain rate (velocity), and recent strain history (Josephson, 1993, 1999; Marsh, 1999). Muscle shortening early in a contraction leads to reduced force later in the contraction (shortening force depression), whereas prior stretch has the opposite effect (lengthening force enhancement) (Edman *et al.*, 1978; Edman, 1980; Granzier & Pollack, 1989; Josephson, 1999). Shortening force depression can last for several minutes in isometric preparations, even if muscle stimulation is disrupted for 1-2s (Granzier & Pollack, 1989).

To distinguish potential instantaneous and history-dependent intrinsic factors, we divided the analysis into two periods, pre-stance and stance, and made measurements at several time points. The pre-stance period was the 2nd half of the swing phase, and in U trials this was extended by the tissue-break through period of the perturbation (Fig. 1). Measurements of strain and velocity at the time of peak force correspond to instantaneous intrinsic factors. We also measured values of muscle fascicle strain and velocity before stance and during stance force development as potential strain history factors. The specific variables measured were: peak force before stance ($F_{pk,\,prior}$) and during stance ($F_{pk,stance}$); muscle fascicle strain and velocity at peak stance phase force (L_{pkF} , V_{pkF}); fascicle strain at 50% stance peak force (L_{Ft50}); mean velocity between TD and 50% stance peak force (V_{Ft50}); the fractional fascicle length change from force onset to the beginning of stance (ΔL_{prior}); total EMG intensity before stance, during stance and over the entire stride ($E_{prior} + E_{stance} = E_{tot}$); and net work before stance, during stance and over the stride ($W_{prior} + W_{stance} = W_{tot}$). Throughout the text, average values for level running are indicated with a subscript ‘c’.

Statistics

Values in the text and figures are the mean and standard deviation (SD) across individuals (N=6), unless otherwise noted. All statistics were calculated using custom software written to use the statistics toolbox in MATLAB (v7, Mathworks, Inc.; Natick, MA, USA). To test for significant differences among the stride categories in the measured variables, we used mixed model ANOVA with stride category (Stride) as a fixed factor and individual (Ind) as a random factor with critical significance level, $\alpha = 0.05$ ('anovan', MATLAB statistical toolbox). Stride categories were coded as follows: U strides were broken into four categories based on sequence (Strides -1, 0, +1 and +2), and C Stride 0 was included as a fifth category. This resulted in a total sample size of 70 with the following degrees of freedom: Stride (X1) = 4, Ind (X2) = 5, X1*X2 = 20, and Error = 39. We used the false discovery rate (FDR) procedure to control the proportion of false positives ($q = 0.05$) over multiple simultaneous tests while maintaining statistical power (Benjamini & Hochberg, 1995; Curran-Everett, 2000). If the full model was significant after FDR correction, we used posthoc t-tests with Bonferroni correction to compare pairs of stride categories. We used a Bonferroni corrected threshold p-value of 0.005 to maintain an error rate $\alpha = 0.05$ for the family of 10 possible pair-wise comparisons within each ANOVA.

We also used the same mixed model ANOVA methods to analyse the leg posture at the time of ground contact: leg length at TD, leg angle at TD, and hip height at TD. These data were available for C Stride 0, U Stride 0 and Stride +1. The leg was in view for fewer than half of U Stride -1, and none of U Stride +2; so these strides were omitted, resulting in 3 stride categories. This resulted in a total sample size of 42 with the following degrees of freedom: Stride (X1) = 2, Ind (X2) = 5, X1*X2 = 10, and Error = 25.

Results:

Altered force, length and work dynamics of the gastrocnemius in the perturbed stride

In the perturbed stride (U Stride 0), the gastrocnemius (G) exhibited large, rapid changes in mechanical output (Fig. 1). The force-length dynamics of the perturbed stride varied considerably (Fig. 2). Nonetheless, several aspects of the force-length dynamics in U Stride 0 were consistent across trials and differed significantly from C trials. In the description of the G perturbation response below, the values reported are the least squared mean difference from C trials, from the ANOVA results (Table 1 C).

An earlier study on joint mechanics during this perturbation revealed that the ankle extends as the foot breaks through the tissue in U Stride 0, (Daley et al., 2007). In the current study, G muscle-tendon force dropped rapidly during this perturbation period, and the LG fascicles shortened until the foot contacted the ground below (Figs. 1 and 2). The gastrocnemius produced positive work throughout the perturbation period. In the extended time period before ground contact in U strides, the muscle underwent -0.29L_o greater fascicle shortening and produced +3.8 Jkg^{-1} more positive work than in the pre-stance period of C strides (ΔL_{prior} and W_{prior}, Table 1 C, Stride 0).

After the tissue breakthrough phase of the perturbation, the leg is reloaded as it contacts the ground below (Daley & Biewener, 2006). The LG underwent stretch during the first part of stance following the perturbation, rather than shortening during the first part of stance, as in level running (Figs. 1 and 2). The muscle redeveloped force during the stance period, but the peak force ($F_{pk,stance}$) was substantially lower than in C strides (Fig. 3, Table 1, Stride 0). Due to shortening during the perturbation, the LG was -0.17 L_o shorter during stance force development (L_{Ft50}, Table 1C, Stride 0). The LG underwent stretch during force development, and muscle length at the time of peak force (L_{pkF}) did not differ significantly from C trials (Table 1C, Stride 0). At the time of $F_{pk,\ stance}$ in U trials, the LG underwent stretch at a rate of +2.4 Ls^{-1}, whereas in C trials the LG shortened at -2.7 Ls^{-1}, a mean difference in fascicle velocity of 5.1 Ls^{-1} between C and U trials (V_{pkF}, Table 1C, Stride 0). The changes in force-length dynamics resulted in a substantially lower stance net work (W_{stance}) following the drop perturbation (Table 1, Fig. 3, Stride 0). Although the gastrocnemius produced +3.8 Jkg^{-1} greater work before stance (W_{prior}), it produced -9.1 Jkg^{-1} less work during stance, for a net difference of -5.2 Jkg^{-1} compared to level running (Table 1). The change in net work was similar in magnitude to the increase in gastrocnemius work observed when the birds run up a 16° incline (+4.3 Jkg^{-1}) (Daley & Biewener, 2003).

Activation changes and reflex latency of the gastrocnemius

Although muscle work and force in the perturbed stride differed significantly from level running, average total EMG intensity (E_{tot}) did not (Table 1, Fig. 3, Stride 0). The average E_{tot} in U trials was slightly greater than C trials; however, this difference was not statistically significant (Fig. 3, Table 1). In many trials, the magnitude of muscle activity differed significantly for short periods of time within the stride (Fig. 2); however the differences were small and variable in timing. Most trials resembled the first two examples in Figure 2 (A and B), in which the time-course and magnitude of

406 muscle activity are similar to that of level running despite large changes in muscle strain and
407 muscle-tendon force.
408
409 Here the animals ran at relatively high speeds: v = 2.6 (0.1) ms^{-1} in C trials and 2.7(0.2) ms^{-1} in U
410 trials (mean(SD)), corresponding to dimensionless speeds, $\hat{u}$, of 1.45 and 1.52, respectively
411 ($\hat{u} = v/(\boldsymbol{g}h)^{\wedge 0.5}$) where $\hat{u}$ is dimensionless speed, h is standing hip height, and $\boldsymbol{g}$ is acceleration due to
412 gravity (Alexander, 1989; Gatesy & Biewener, 1991). A tendon tap test performed on the Achilles
413 tendon suggests a transmission delay for the stretch reflex of 6(2) ms in the guinea fowl
414 gastrocnemius, when measured as the time between fascicle stretch and EMG spike (Nishikawa et
415 al., 2007). Cross-correlation between the force and EMG intensity traces in level running suggests a
416 lag of 34(5) ms between activation and force development (with a correlation coefficient of
417 0.88(0.02)). This suggests a total reflex latency of approximately 40 ms, 34% of mean stance period
418 in C trials (118 ms). Most of the change in muscle-tendon force occurs earlier than this, suggesting
419 an intrinsic mechanical cause (Figs. 1 and 2). Trials with larger changes in EMG activity within the
420 perturbed stride also happened to be trials at the low end of the speed range (see Fig. 2 C, v = 2.3
421 ms^{-1}, $\hat{u}$ = 1.2).
422
423 *Muscle performance and recovery following the perturbation*
424 The bird did not completely recover within the perturbed stride, but likely recovered by the end of
425 the 2nd stride following the perturbation. In the 1st stride following the perturbation (Stride +1), the
426 bird stepped back up (8.5 cm) to the original level of the platform (Figs. 1 and 2). The bird's leg
427 contacted the ground with a crouched posture during this stride (Fig. 1, Table 2). Muscle work, peak
428 force and total EMG intensity were all significantly greater in Stride +1 than C strides (Table 1, Fig.
429 3). By the 2nd stride following the drop (Stride +2), however, 12 of the 13 variables were not
430 significantly different from C strides, although there was a significant decrease in net muscle work
431 compared to level trials (Table 1).
432
433 *Muscle mechanical output correlates with altered leg posture*
434 The force and work output of the gastrocnemius was correlated with leg posture at the start of the
435 stance phase. Peak muscle force and net mechanical work during stance were inversely correlated
436 with hip height at the time of foot contact (Fig. 4, reduced major axis regression) (page 544 Sokal &
437 Rohlf, 1995). A similar relationship held for both the perturbed stride (Stride 0) and the first
438 recovery stride (Stride +1). Hip height (H) represents the overall leg posture, which is a function of

both effective leg length and leg contact angle (H = leg length*sine (leg angle)), which both differed significantly from level running in U Stride 0 and U Stride +1 (Table 2). In U Stride 0, the change in hip height is primarily due to a change in contact angle (Table 2), which is likely due to increased hip and ankle extension (Daley et al. 2007). In U Stride +1, the change in hip height receives roughly equal contribution from altered effective leg length and contact angle. Joint kinematics have not been studied in detail for the step up, but the altered posture is likely associated with increased flexion of the knee and ankle (Fig. 1). The more extended, retracted leg posture in U Stride 0 was associated with reduced force and work output, whereas the flexed, crouched posture in U Stride +1 was associated with higher force and work output. This pattern mirrors the leg posture-dependent mechanics of the whole leg, and likely reflects intrinsic geometry factors of limb posture on limb loading during stance (Daley & Biewener, 2006).

Discussion:

The role of distal hindlimb muscles in perturbation recovery and stability

A previous study revealed that guinea fowl achieve impressive stability following this unexpected perturbation, rarely stumbling and maintaining the same average speed despite a drop in the support surface of 40% leg length (Daley et al., 2006). The stabilising mechanisms include intrinsic mechanical changes in leg loading that result from altered leg posture during stance (Daley & Biewener, 2006). Joint mechanics during the perturbation suggest that the distal hindlimb extensor muscles play a key role in the posture-dependent stabilising response (Daley et al., 2007). External joint work at the distal joints changes rapidly in response to altered leg posture and loading during the perturbation, whereas that of the proximal joints (hip and knee) remains similar to level running (Daley et al., 2007).

The current results indicate, as suggested by external joint mechanics, that the perturbation leads to rapid, intrinsic changes in force-length dynamics and net work output by the gastrocnemius. The change in mass-specific work is similar in magnitude to that observed during steady incline running (Daley & Biewener, 2003; Gabaldon *et al.*, 2004). Muscle force and work following the perturbation are strongly correlated with leg posture (Fig. 4), mirroring the posture-sensitive limb and joint mechanics observed in the previous studies described above.

In considering the implications of gastrocnemius force-length performance for running stability, it is helpful to review three hypothetical strategies for handling a substrate height perturbation (also

discussed in: Daley & Biewener, 2006; Daley *et al.*, 2006). Here we define a stable response as any that allows the bird to return to steady forward locomotion after a transient recovery period (without a fall or injury). To achieve this, the animal can: 1) prevent change in body height and velocity despite a change in terrain, by adjusting effective leg length and stiffness appropriately (maintaining spring-like mechanics), 2) passively redistribute energy between gravitational potential energy and kinetic energy by using spring-like or strut-like leg mechanics, or 3) produce or absorb energy to adjust body height to the new terrain height while maintaining constant velocity (as if moving up or down stairs or a slope). It is possible for an animal to use each of the mechanisms alone, or achieve a range of behaviours by combining them. A simple mass-spring model (with no ability to produce or absorb mechanical energy) can use the first two of these mechanisms to maintain stability following a change in terrain height (Seyfarth et al., 2003). However, it is unknown how large a substrate height perturbation can be successfully handled in such a passive manner.

If the animal could anticipate the change in terrain height, it might choose among these mechanisms based on context and the desired outcome. For example, it may use a spring-like mechanism to deal with a single step change and immediately return to the original terrain height, and use an energy producing or absorbing mechanism to adjust body height and maintain constant velocity at a new terrain height.

The unexpected drop perturbation led to a range of behaviour depending on the interaction between the neuromuscular activity, joint dynamics, leg posture and the ground. This variation reveals that the gastrocnemius exhibits an inherently stable context-dependent response. In the drop step, the leg contacts the ground with a more extended posture than 'normal' (compared to the C average: Table 2, Fig. 4), and gastrocnemius force and work output decrease (with no change in EMG intensity) (Fig. 3). The leg absorbs energy, leading toward a normal posture at the lower substrate height and minimising acceleration of the body. In the recovery step up, the leg contacts the ground with a more crouched posture than normal (Table 2, Fig. 4) and gastrocnemius force and work output increase (associated with increased EMG intensity by this point in time) (Fig. 3). This helps to increase the total mechanical energy of the body, again pushing the bird toward steady running with a normal leg posture. This relationship between leg posture and gastrocnemius work output may help prevent the bird from reaching extremes in leg and body posture that would lead to a fall, facilitating a stable recovery from a perturbation. The rapid changes in G muscle work involved in

this response are likely inherently linked to the intrinsic strain- and load-dependent contractile properties of muscle, as discussed below.

Muscle-tendon architecture and function for stability

The current results, along with other recent studies, suggest that the mechanical roles of distal hindlimb extensor muscles are broader than previously thought. It has been observed that distal muscles tend to have a distinct architecture: pennate fibre arrangement, long tendon and high ratio of tendon length to fibre length. This architecture is usually interpreted as reflecting function for isometric contraction and limited work, economic body weight support, and elastic energy cycling for steady locomotion. In contrast, muscles with longer, parallel fibre arrangement and little free tendon are thought to be the primary actuators for high mechanical work output (Biewener & Roberts, 2000; Smith *et al.*, 2006; Biewener & Daley, 2007). However, recent studies also suggest that muscles with pennate architecture are capable of a broad range of mechanical roles, including high mechanical work output for incline running and acceleration (Roberts *et al.*, 1997; Roberts & Scales, 2004). Although pennate architecture may limit the stroke length of the muscle actuator, and the frequencies at which a muscle can perform useful work, the total work capacity is proportional to muscle volume, not fibre arrangement (Zajac, 1989; Alexander, 1992). Furthermore, a recent 3D model of muscle shape change during contraction reveals that pennate architecture provides an important mechanism for rapidly changing muscle mechanical output. Pennate fibre arrangement allows variable gearing at the muscle-tendon level depending on loading conditions, which could provide a mechanism for a muscle to rapidly and intrinsically switch among mechanical roles (Azizi et al., 2008). Thus, recent models and experimental results suggest that distal muscles with pennate architecture are capable of rapidly switching between economic force development and high work output, depending on the particular loading conditions encountered during locomotion.

Intrinsic mechanical effects versus reflex modulation of muscle action

The unexpected drop perturbation provides an opportunity to investigate the effect of intrinsic mechanical factors on muscle dynamics. Reflex mediated responses require at least 30-40 ms in these birds, so the immediate response to the perturbation relies entirely on the interplay between intrinsic mechanics and feedforward muscle activation. After this point, it is possible for both intrinsic and reflex mediated factors to contribute to the response. Some variability was recorded in the intensity of muscle activation in the stride just before the perturbation (Stride -1), which may have led to some of the observed variability in the subsequent response. However, the intensity of

muscle activation significantly differed from level running only in the first stride following the perturbation (U Stride +1, Fig. 3). In the perturbed stride (U Stride 0) there was slight tendency for increased muscle activation which was not statistically significant (Table 1). An increase in activation would tend to increase force output, yet we observed an 81% decrease in peak muscle force ($F_{pk,\ stance}$) in U Stride 0 (Table 1). These findings suggests that in U Stride 0 the effect of altered activity on G muscle force is small compared to the effect of intrinsic mechanical factors.

Intrinsic muscle properties and current neuromechanical models

The most likely intrinsic mechanical factors would seem to be the instantaneous force-length and force-velocity properties of muscle, considered primary factors in muscle contractile performance (Josephson, 1999). Most large-scale musculoskeletal simulations use Hill-type muscle models that treat activation, length and velocity as independent, instantaneous factors that influence the force output of a muscle. Thus, the only intrinsic factors in muscle output in these models are instantaneous effects.

The decrease in force during the break-through perturbation occurs simultaneously with increased fascicle shortening, consistent with instantaneous intrinsic factors (Fig. 2). In the subsequent stance phase muscle-tendon force remains low relative to level strides. In the statistical analysis, we have compared muscle force between U and C strides at the time of the stance phase peak ($F_{pk,\ stance}$), when leg is loaded by the body, although these occur at different absolute times relative to stance onset. This shows that $F_{pk,\ stance}$ is reduced by 81% while the fascicles are at a similar length (L_{pkF}) and undergoing stretch (V_{pkF}) (Table 1, Stride 0).

The statistical results suggest that shortening force depression may be an important contributor to the reduced force output, in addition to the instantaneous length and velocity factors included in standard Hill-type models. The gastrocnemius actively shortens and produces positive work during the tissue-breakthrough period of the perturbation. The muscle undergoes $0.29L_o$ greater shortening (ΔL_{prior}) and $3.8 Jkg^{-1}$ greater positive work (W_{prior}) before stance when compared to level running trials (Table 1). It is well recognised that a muscle's recent contractile history influences contractile performance (Edman et al., 1978; Edman, 1980; Josephson, 1999). In particular, muscle shortening early in a contraction leads to reduced force later in the contraction (Granzier & Pollack, 1989; Josephson, 1999).

History-dependent factors are typically considered secondary and neglected in most large-scale musculoskeletal simulations (Zajac, 1989; Delp & Loan, 1995). Yet, it is well recognised that these effects can be large at submaximal levels of stimulation and when muscle strains are high (Sandercock & Heckman, 1997; Askew & Marsh, 1998; Ahn & Full, 2002; Perreault *et al.*, 2003). Although more complex muscle models may be more accurate, this improved accuracy needs to be weighed against the computational demand of intensive large-scale neuromechanical models. Nevertheless, such effects need to be evaluated and considered in developing improved muscle models. An important challenge for current and future work, therefore, is the refinement of simple muscle models that provide reasonably accurate predictions of dynamic muscle mechanical output over a wide range of locomotor behaviours. Future work should test whether a Hill or modified Hill type model that includes history effects (e.g., Meijer et al. 1998) could provide adequate predictions of stability characteristics during running.

The speed-dependent role of reflexes in locomotion

Taken together, available evidence supports the principle of speed-dependent roles of reflex feedback. Previous perturbation studies suggest that spinal reflexes and higher brain centres contribute to the stabilisation of walking (Gorassini *et al.*, 1994; Hiebert & Pearson, 1999; Marigold & Patla, 2005), whereas our findings indicate that running stabilisation is mediated to a large extent by intrinsic mechanics. Loss of ground support in walking cats leads to reduced extensor muscle activity within the perturbed stance (Hiebert & Pearson, 1999). In contrast, the present perturbation study did not result in a consistent, significant change in muscle activity within the perturbed stride (Fig 3). Evidence for reflex feedback, as suggested by small peaks in myoelectric intensity in the stance following the perturbation (Fig. 2), existed in some cases; however, this was quite variable and not statistically significant across individuals (Fig. 3). Nonetheless, sensory feedback likely plays an important role in regulating muscle recruitment during the first recovery stride, as the intensity of gastrocnemius activity was 2.2-fold higher in the 1st stride recovery following the perturbation (Fig. 3). By this time, a number of neural mechanisms are likely to be involved, including longer latency reflexes and higher brain centres (Dietz, 1996; Pearson et al., 1998). These findings suggest that the role of afferent feedback differs between walking and running, consistent with previous reports that reflex contributions to muscle activity tend to be lower in running than in walking (Capaday & Stein, 1987; Ferris *et al.*, 2001).

Limitations and future directions

In vivo measures of muscle performance provide insight into dynamics of neuromuscular performance that can be difficult or infeasible to obtain through any other currently available approaches. To our knowledge, the current study provides the first direct measures of *in vivo* muscle-tendon force and muscle fascicle length during dynamic stabilisation of running. This approach provides new insight into the likely effects of intrinsic muscle properties, and the functionally relevant strain ranges of muscle during more extreme locomotor conditions. These direct measures can provide a key source of information for cross-validation with neuromuscular simulations and advanced imaging techniques that are increasingly used to predict and measure dynamic muscle performance.

These *in vivo* measures also present a number of challenges and limitations that should be kept in mind when interpreting the results. *In vivo* techniques currently allow measurement of a limited number of muscles, because tendon buckles can be used only on muscles with long free tendons. Furthermore, only a limited number of sonomicrometry transducers can feasibly be implanted at a time. The current study required that all of the transducers operate successfully in somewhat extreme conditions of rapid locomotion with large perturbations that induce high strains. To gain insight into the intrinsic mechanics, the experiment required that the perturbation be a surprise, which severely limited the sample size. To minimise complexity and allow comparison to previous studies of *in vivo* gastrocnemius function, we implanted single pair of sonomicrometry crystals in the middle of the muscle belly (Roberts *et al.*, 1997; Daley & Biewener, 2003; Gabaldon *et al.*, 2004). Similar to these earlier studies, we have assumed that recordings from a single location reasonably represent the average fascicle strains of the whole muscle. Consequently, the measurements here do not account for heterogeneity within the muscle (Ahn et al., 2003; Higham et al., 2008), fiber rotation during contraction (Herbert & Gandevia, 1995) or more complex 3D shape changes that could lead to load dependent fiber rotation and dynamically variable architectural gear ratio (Azizi et al., 2008). These factors could alter estimates of fascicle strain and force, and are likely to be important for understanding the relationship between muscle-tendon architecture, intrinsic mechanics and muscle performance in more detail. Consequently, these issues should be addressed by future work.

Nonetheless, although these factors would influence the accuracy of our force and work estimates, it is unlikely to change the main findings and conclusions. This perturbation is quite large, and has

similar effects on loading across all hindlimb joints (Daley et al., 2007). Recent work has demonstrated distinct function in the lateral and medial heads of the gastrocnemius, likely because these bi-articular muscles are antagonists at the knee in birds (Higham et al., 2008). Nonetheless, all heads of the gastrocnemius have a similar overall function: they are activated with similar timing just before stance and develop force through most of the stance phase (Higham et al., 2008). Furthermore, the drop perturbation was found to have a larger effect on ankle joint work than knee joint work (Daley et al., 2007), where all heads of the gastrocnemius synergistically converge onto a common tendon. Consequently, the changes in mechanical work during the perturbation are likely to be similar in polarity (although perhaps not absolute magnitude) among all gastrocnemius heads. Consequently, heterogeneity within the muscle group would likely influence the magnitude of the work estimates, but are unlikely to change the qualitative assessment of the findings.

Conclusions

I*n vivo* studies of muscle function suggest that the gastrocnemius muscle is capable of playing a number of important roles in running, including both economic performance in steady running and rapid bursts of high work output for stabilisation tasks. Our current findings, combined with other recent studies of muscle function, highlight the importance of understanding the interplay of mechanical structure and neuromuscular control. Neural commands must be filtered through musculoskeletal architecture, which can either limit or amplify the neural signal. Appropriate integration of mechanics and control may minimise the need for active neural compensation to recover from unexpected changes in terrain. In running, the interplay of environmental interaction, leg mechanics and muscle mechanics may, at least initially, mediate most of the response to a sudden change in terrain. In light of previous findings in studies on walking, the results here support the concept of speed-dependent roles of reflex feedback. The findings also suggest the potential need for incorporating history-dependent muscle properties into neuromechanical models that seek to simulate high speed locomotion, especially if high muscle strains are involved and stability characteristics are important.

Author contributions: MAD designed the experiment, analysed and interpreted the data, drafted and revised the article, AS assisted in data analysis and interpretation and revising of the article, AAB was involved in experimental design, data interpretation and critical revision of the article. All authors approved the final version.

Acknowledgements:

We thank the numerous colleagues at the Concord Field Station of Harvard University, including Craig McGowan, Jim Usherwood, Polly McGuigan, Russ Main, Ed Yoo, for providing advice, assistance and feedback at various stages of this work, as well as Mr. Pedro Ramirez for care of animals. Dr. James Wakeling provided advice and MATLAB code for the wavelet analysis of EMG data. We are also grateful to members of the Human Neuromechanics Laboratory at the University of Michigan for helpful discussions. This work was supported by an HHMI Predoctoral Fellowship and an NSF Bioinformatics Postdoctoral Fellowship to MAD (DBI-0630664), and an NIH grant (AR047679) to AAB.

679

Table 1. Muscle variables measured for analysis. **A**) Mean and standard deviation across individuals for level running (C Stride 0). **B**) P-values for the mixed model ANOVA test for the effect of 'Stride Category', after FDR correction for multiple ANOVA tests. **C**) Post-hoc multiple comparisons between U strides and C Stride 0. Value indicates the least-squared mean difference from C Stride 0, in normalised units shown in **B**. Bolding indicates significance based on a Bonferroni threshold of p = 0.005. See methods.

A) Level running means

Variable	Mean (SD)
$F_{pk,\ prior}$ (N)	11.7 (2.8)
$F_{pk,\ stance}$ (N)	59.7 (2.5)
W_{prior} (Jkg^{-1})	1.7 (0.3)
W_{stance} (Jkg^{-1})	8.2 (1.1)
W_{tot} (Jkg^{-1})	10.0 (1.2)
V_{Ft50} (Ls^{-1})	-9.9 (2.9)
V_{pkF} (Ls^{-1})	-2.7 (0.4)
L_{Ft50}	1.17 (0.04)
L_{pkF}	1.10 (0.02)
ΔL_{prior}	-0.52 (0.16)
E_{prior} (E/E_{tot})	0.5 (0.1)
E_{stance} (E/E_{tot})	0.5 (0.1)

B) ANOVA results

Variable	P-value
$F_{pk,\ prior}$ ($F/F_{pk,c}$)	**< 0.0001**
$F_{pk,\ stance}$ ($F/F_{pk,c}$)	**< 0.0001**
W_{prior} ($W\text{-}W_c$, Jkg^{-1})	**< 0.0001**
W_{stance} ($W\text{-}W_c$, Jkg^{-1})	**< 0.0001**
W_{tot} ($W\text{-}W_c$, Jkg^{-1})	**< 0.0001**
V_{Ft50} ($V\text{-}V_c$, Ls^{-1})	**0.0015**
V_{pkF} ($V\text{-}V_c$, Ls^{-1})	**0.0073**
L_{Ft50} ($L\text{-}L_c$)	**< 0.0001**
L_{pkF} ($L\text{-}L_c$)	**0.0002**
ΔL_{prior}	**0.0001**
E_{prior} ($E/E_{tot,c}$)	**0.0015**
E_{stance} ($E/E_{tot,c}$)	**0.0049**
E_{tot} ($E/E_{tot,c}$)	**0.0013**

C) Normalised least-squared mean difference from C

Stride -1	Stride 0	Stride +1	Stride +2
0.03	**0.42**	**0.16**	-0.02
-0.01	**-0.81**	**0.60**	-0.13
0.4	**3.8**	-2.1	-1.0
-0.7	**-9.1**	**11.9**	-3.7
-0.4	**-5.2**	**9.8**	**-4.7**
-3.7	**7.2**	-4.0	-3.0
0.7	**5.1**	**-2.1**	1.8
0.01	**-0.17**	**0.27**	-0.01
0.00	-0.06	**0.20**	0.01
-0.04	**-0.29**	**0.33**	0.04
0.2	**0.7**	0.4	-0.1
0.0	-0.4	**0.8**	-0.2
0.2	0.3	**1.2**	-0.3

680
681

682

Table 2. ANOVA results for leg posture variables at the time of toe contact with the ground (TD) for the strides in which kinematics were consistently available. Hip height (H) is a function of both effective leg length and leg angle ($H = L_{leg}$*sine(leg angle)). Bolded values indicate statistically significant difference from C Stride 0 at a Bonferroni threshold of p = 0.0167.

Variable	p-value	C Stride 0	Stride 0	Stride +1
Leg length at TD (L/H_c)	**0.0015**	1.32 (0.06)	**1.39 (0.07)**	**1.20 (0.10)**
Leg angle at TD (degrees)	**< 0.0001**	49.7 (2.8)	**72.8 (8.9)**	**37.6 (6.5)**
Hip height at TD (H/H_c)	**< 0.0001**	1.00 (0.05)	**1.31 (0.08)**	**0.73 (0.14)**

683
684

Figure legends:

Figure 1. Muscle recordings from the gastrocnemius as a guinea fowl encounters and recovers from a sudden drop on terrain while running. Fascicle length (top trace) and EMG activity (bottom trace) were recorded from the lateral head of the gastrocnemius (LG), and muscle-tendon force (middle trace) was recorded from the common gastrocnemius tendon (G). Stance periods are indicated by gray boxes. The bird encounters an unexpected 8.5 cm drop in terrain height at Stride 0, and steps back up to the original platform height at Stride +1. We analysed strides from the Stride prior (Stride -1), to the second recovery stride following the drop (Stride +2). The coloured bars for the stride sequence indicate the colour coding used in subsequent figures. Silhouettes across the top schematically illustrate the position of the recording limb at the time points indicated by the gray vertical lines. In the perturbed stride the time of foot contact with the tissue paper is shown with a dashed line, followed by time of foot contact with the actual ground indicated by the solid line.

Figure 2. LG fascicle length, G muscle-tendon force and LG EMG intensity, comparing the U perturbed trial Stride 0 (top) and Stride +1 (bottom) to steady level running. In gray, the mean±95% confidence interval for level running is shown for each trace, averaged across all 12 C strides per individual (Stride -1 to Stride +2 for 3 trials). A single example is overlaid from a U trial perturbed stride (U Stride 0, top, thick red line) and first recovery stride (U Stride +1, bottom, thick green line). Examples are shown from three different individuals in columns A, B and C, which span the range of U responses observed. The middle example (**B**, Ind 6) was nearest the mean across individuals for muscle force-length values and running speed (v = 2.7 ms^{-1}). The bird in **A** ran faster than average (v = 3.1 ms^{-1}), and the bird in **C** ran slower than average (v = 2.3 ms^{-1}). The stance period for the perturbed stride is indicated by the gray box, and the average stance period for level running by the dashed vertical lines. In the top traces, the first dashed line also corresponds to the time of tissue paper contact in the perturbed stride (and presumably the anticipated start of stance).

Figure 3. The mean ($\pm$ SD) values across individuals for stance peak muscle-tendon force ($F_{pk,stance}$), muscle work during stance (W_{stance}) and total EMG intensity (E_{tot}), for each stride in the sequence encountering and recovering from the perturbation (Stride -1 to Stride +2). All variables are shown relative to the mean for C trials as indicated in the labels. Asterisks indicate a statistically significant difference from level running (Table 1). Colours as indicated in Figure 1.

Figure 4. Muscle mechanical output in relation to leg posture. **A**) Peak muscle force ($F_{pk,stance}$) and **B)** muscle work during stance (W_{stance}) inversely correlate with the relative extension of the leg, measured as hip height at the time of toe down (TD; when the foot first touches the true ground level). Hip height serves as a general proxy for leg posture: when the foot is either more extended or at a steeper angle (closer to vertical), hip height is higher (see Table 2). This is also associated with a more extended ankle (Daley et al. 2007). Data shown are for level running (C), the unexpected drop (Stride 0), and the subsequent step up (Stride +1). The silhouettes schematically illustrate typical leg postures for each condition. The solid black line is the reduced major axis regression fit, with equation of the line and R-squared value shown. Gray dashed lines indicate the mean for level running.

References:

Ahn AN & Full RJ. (2002). A motor and a brake: two leg extensor muscles acting at the same joint manage energy differently in a running insect. *J Exp Biol* **205,** 379-389.

734 Ahn AN, Monti RJ & Biewener AA. (2003). In vivo and in vitro heterogeneity of segment length changes in
735 the semimem branosus muscle of the toad. *J Physiol* **549,** 877-888.
736
737 Alexander RM. (1989). Optimization and gaits in the locomotion of vertebrates. *Physiol Rev* **69,** 1199-1227.
738
739 Alexander RM. (1992). The work that muscles can do. *Nature* **357,** 360.
740
741 Askew GN & Marsh RL. (1998). Optimal shortening velocity (V/Vmax) of skeletal muscle during cyclical
742 contractions: length-force effects and velocity-dependent activation and deactivation. *J Exp Biol* **201,**
743 1527-1540.
744
745 Azizi E, Brainerd EL & Roberts TJ. (2008). Variable gearing in pennate muscles. *Proc Natl Acad Sci U S A*
746 **105,** 1745-1750.
747
748 Benjamini Y & Hochberg Y. (1995). Controlling the False Discovery Rate: A Practical and Powerful
749 Approach to Multiple Testing. *J Roy Stat Soc B Met* **57,** 289-300.
750
751 Biewener AA & Corning WR. (2001). Dynamics of mallard (Anas platyrhynchos) gastrocnemius function
752 during swimming versus terrestrial locomotion. *J Exp Biol* **204,** 1745-1756.
753
754 Biewener AA & Daley MA. (2007). Unsteady locomotion: integrating muscle function with whole body
755 dynamics and neuromuscular control. *J Exp Biol* **210,** 2949-2960.
756
757 Biewener AA, Konieczynski DD & Baudinette RV. (1998). In vivo muscle force-length behavior during
758 steady speed hopping in tammar wallabies. *J Exp Biol* **201,** 1681-1694.
759
760 Biewener AA & Roberts RJ. (2000). Muscle and tendon contributions to force, work, and elastic energy
761 savings: A comparative perspective. *Exerc Sport Sci Rev* **28,** 99-107.
762
763 Brown IE & Loeb GE. (2000). A reductionist approach to creating and using neuromechanical models. In
764 *Biomechanics and Neural Control of Posture and Movement*, ed. Winters JM & Crago PE, pp. 148-
765 163. Springer-Verlag, New York.
766
767 Capaday C & Stein RB. (1987). Difference in the amplitude of the human soleus H reflex during walking and
768 running. *J Physiol* **392,** 513-522.
769
770 Curran-Everett D. (2000). Multiple comparisons: philosophies and illustrations. *Am J Physiol Regul Integr*
771 *Comp Physiol* **279,** R1-8.
772
773 Daley MA & Biewener AA. (2003). Muscle force-length dynamics during level versus incline locomotion: a
774 comparison of in vivo performance of two guinea fowl ankle extensors. *J Exp Biol* **206,** 2941-2958.
775
776 Daley MA & Biewener AA. (2006). Running over rough terrain reveals limb control for intrinsic stability.
777 *Proc Natl Acad Sci U S A* **103,** 15681-15686.
778
779 Daley MA, Felix G & Biewener AA. (2007). Running stability is enhanced by a proximo-distal gradient in
780 joint neuromechanical control. *J Exp Biol* **210,** 383-394.
781
782 Daley MA, Usherwood JR, Felix G & Biewener AA. (2006). Running over rough terrain: guinea fowl
783 maintain dynamic stability despite a large unexpected change in substrate height. *J Exp Biol* **209,**
784 171-187.
785
786 Delp SL & Loan JP. (1995). A Graphics-Based Software System to Develop and Analyze Models of
787 Musculoskeletal Structures. *Comput Biol Med* **25,** 21-34.

Dickinson MH, Farley CT, Full RJ, Koehl MAR, Kram R & Lehman S. (2000). How animals move: an integrative view. *Science* **288,** 100-106.

Dietz V. (1996). Interaction between central programs and afferent input in the control of posture and locomotion. *J Biomech* **29,** 841-844.

Dietz V, Quintern J & Sillem M. (1987). Stumbling Reactions in Man - Significance of Proprioceptive and Pre-Programmed Mechanisms. *J Physiol* **386,** 149-163.

Edman KAP. (1980). Depression of mechanical performance by active shortening during twitch and tetanus of vertebrate muscle fibres. *Acta Physiol Scand* **109,** 15-26.

Edman KAP, Elzinga G & Noble MIM. (1978). Enhancement of mechanical performance by stretch during tetanic contractions of vertebrate skeletal muscle fibres. *J Physiol* **281**.

Ferris DP, Aagaard P, Simonsen EB, Farley CT & Dyhre-Poulsen P. (2001). Soleus H-reflex gain in humans walking and running under simulated reduced gravity. *J Physiol* **530,** 167-180.

Gabaldon AM, Nelson FE & Roberts TJ. (2004). Mechanical function of two ankle extensors in wild turkeys: shifts from energy production to energy absorption during incline versus decline running. *J Exp Biol* **207,** 2277-2288.

Gatesy SM & Biewener AA. (1991). Bipedal locomotion: effects of speed, size and limb posture in birds and humans. *J Zool Lond* **224,** 127-147.

Gorassini MA, Prochazka A, Hiebert GW & Gauthier MJA. (1994). Corrective Responses to Loss of Ground Support During Walking .1. Intact Cats. *J Neurophysiol* **71,** 603-610.

Granzier HL & Pollack GH. (1989). Effect of active pre-shortening on isometric and isotonic performance of single frog muscle fibres. *J Physiol* **415,** 299-327.

Herbert RD & Gandevia SC. (1995). Changes in pennation with joint angle and muscle torque: in vivo measurements in human brachialis muscle. *J Physiol* **484,** 523-532.

Hiebert GW, Gorassini MA, Jiang W, Prochazka A & Pearson KG. (1994). Corrective Responses to Loss of Ground Support During Walking .2. Comparison of Intact and Chronic Spinal Cats. *J Neurophysiol* **71,** 611-622.

Hiebert GW & Pearson KG. (1999). Contribution of sensory feedback to the generation of extensor activity during walking in the decerebrate cat. *J Neurophysiol* **81,** 758-770.

Higham TE, Biewener AA & Wakeling JM. (2008). Functional diversification within and between muscle synergists during locomotion. *Biology Letters* **4,** 41-44.

Jindrich DL & Full RJ. (2002). Dynamic stabilization of rapid hexapedal locomotion. *J Exp Biol* **205,** 2803-2823.

Josephson RK. (1993). Contraction Dynamics and Power Output of Skeletal Muscle. *Annu Rev Physiol* **55,** 527-546.

Josephson RK. (1999). Dissecting muscle power output. *Journal of Experimental Biology* **202,** 3369-3375.

Kubow TM & Full RJ. (1999). The role of the mechanical system in control: a hypothesis of self-stabilization in hexapedal runners. *Philos Trans R Soc Lond B Biol Sci* **354,** 849-861.

Lichtwark GA & Wilson AM. (2006). Interactions between the human gastrocnemius muscle and the Achilles tendon during incline, level and decline locomotion. *J Exp Biol* **209,** 4379-4388.

Marigold DS & Patla AE. (2005). Adapting locomotion to different surface compliances: Neuromuscular responses and changes in movement dynamics. *J Neurophysiol* **94,** 1733-1750.

Marsh RL. (1999). How muscles deal with real-world loads: The influence of length trajectory on muscle performance. *J Exp Biol* **202,** 3377-3385.

McGowan CP, Duarte HA, Main JB & Biewener AA. (2006). Effects of load carrying on metabolic cost and hindlimb muscle dynamics in guinea fowl (Numida meleagris). *J Appl Physiol* **101,** 1060-1069.

McGowan CP, Neptune RR & Kram R. (2008). Independent effects of weight and mass on plantar flexor activity during walking: implications for their contributions to body support and forward propulsion. *Journal of Applied Physiology* **105,** 486-494.

Moritz CT & Farley CT. (2004). Passive dynamics change leg mechanics for an unexpected surface during human hopping. *J Appl Physiol* **97,** 1313-1322.

Nichols TR. (1994). A biomechanical perspective on spinal mechanisms of coordinated muscular action: an architecture principle. *Acta Anat (Basel)* **151,** 1-13.

Nichols TR & Houk JC. (1973). Reflex Compensation for Variations in the Mechanical Properties of a Muscle. *Science* **181,** 182-184.

Nishikawa K, Biewener AA, Aerts P, Ahn AN, Chiel HJ, Daley MA, Daniel TL, Full RJ, Hale ME, Hedrick TL, Lappin AK, Nichols TR, Quinn RD, Satterlie RA & Szymik B. (2007). Neuromechanics: an integrative approach for understanding motor control. *Integr Comp Biol* **47,** 16-54.

Patla AE & Prentice SD. (1995). The role of active forces and intersegmental dynamics in the control of limb trajectory over obstacles during locomotion in humans. *Exp Brain Res* **106,** 499-504.

Pearson K, Ekeberg O & Buschges A. (2006). Assessing sensory function in locomotor systems using neuro-mechanical simulations. *Trends Neurosci* **29,** 625-631.

Pearson KG, Misiaszek JE & Fouad K. (1998). Enhancement and resetting of locomotor activity by muscle afferents. In *Neuronal Mechanisms for Generating Locomotor Activity*, ed. Kiehn O, Harris-Warrick RM, Jordan LM, Hultborn H & Kudo N, pp. 203-215.

Perreault EJ, Heckman CJ & Sandercock TG. (2003). Hill muscle model errors during movement are greatest within the physiologically relevant range of motor unit firing rates. *J Biomech* **36,** 211-218.

Prilutsky BI, Herzog W & Allinger TL. (1996). Mechanical power and work of cat soleus, gastrocnemius and plantaris muscles during locomotion: possible functional significance of mucle design and force patterns. *J Exp Biol* **199,** 801-814.

Roberts TJ, Kram R, Weyand PG & Taylor CR. (1998). Energetics of bipedal running I. Metabolic cost of generating force. *J Exp Biol* **201,** 2745-2751.

Roberts TJ, Marsh RL, Weyand PG & Taylor CR. (1997). Muscular force in running turkeys: the economy of minimizing work. *Science* **275,** 1113-1115.

Roberts TJ & Scales JA. (2004). Adjusting muscle function to demand: joint work during acceleration in wild turkeys. *J Exp Biol* **207,** 4165-4174.

Sandercock TG & Heckman CJ. (1997). Force From Cat Soleus Muscle During Imposed Locomotor-Like Movements: Experimental Data Versus Hill-Type Model Predictions. *J Neurophysiol* **77,** 1538-1552.

Seyfarth A, Geyer H & Herr H. (2003). Swing-leg retraction: a simple control model for stable running. *J Exp Biol* **206,** 2547-2555.

Smith NC, Wilson AM, Jespers KJ & Payne RC. (2006). Muscle architecture and functional anatomy of the pelvic limb of the ostrich (Struthio camelus). *J Anat* **209,** 765-779.

Sokal RR & Rohlf FJ. (1995). *Biometry: the principles and practice of statistics in biological research*. W. H. Freeman and Co., New York.

Sponberg S & Full RJ. (2008). Neuromechanical response of musculo-skeletal structures in cockroaches during rapid running on rough terrain. *J Exp Biol* **211,** 433-446.

von Tscharner V. (2000). Intensity analysis in time-frequency space of surface myoelectric signals by wavelets of specified resolution. *J Electromyogr Kinesiol* **10,** 433-445.

Wakeling JM, Kaya M, Temple GK, Johnston IA & Herzog W. (2002). Determining patterns of motor recruitment during locomotion. *J Exp Biol* **205,** 359-369.

Zajac FE. (1989). Muscle and Tendon - Properties, Models, Scaling, and Application to Biomechanics and Motor Control. *Crit Rev Biomed Eng* **17,** 359-411.

Figure 1

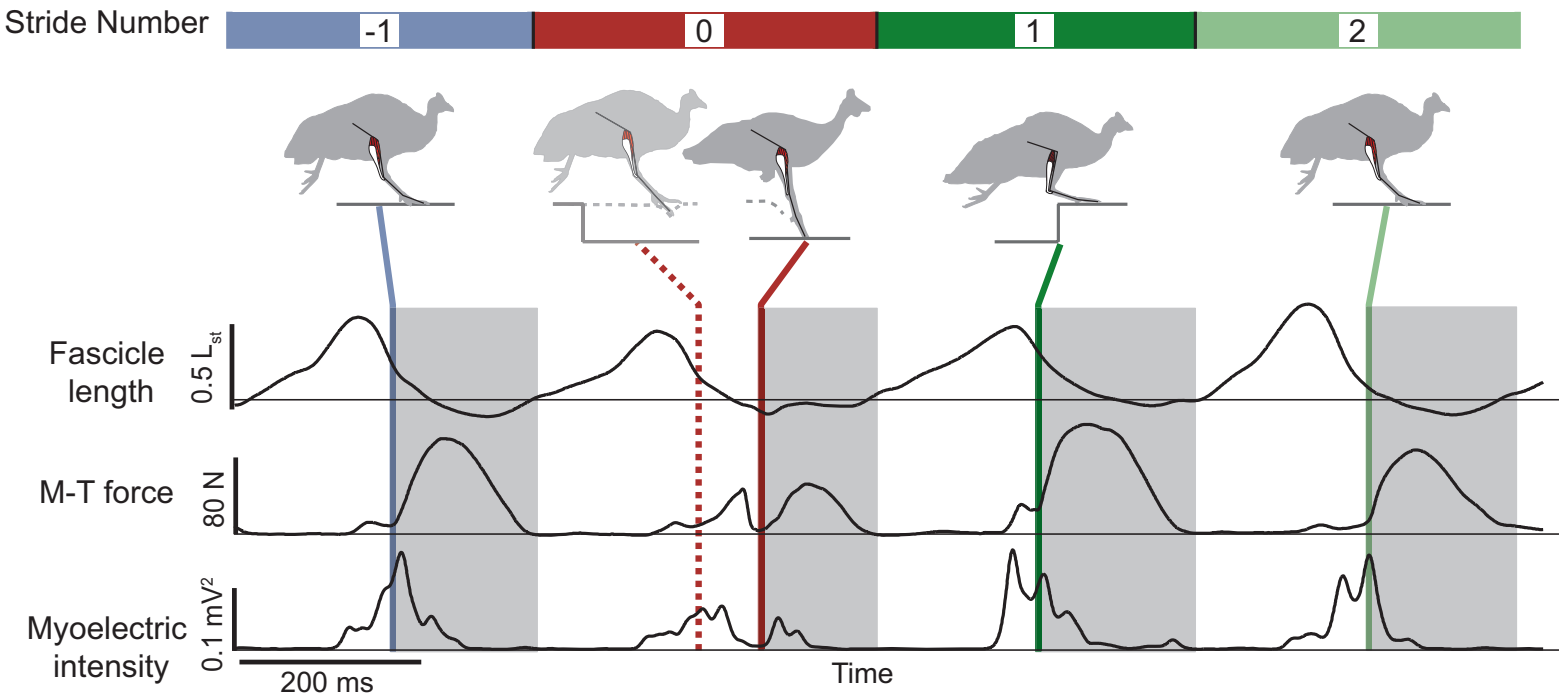
Stride Number
-1
0
1
2
Fascicle length
0.5 L_{st}
M-T force
80 N
Myoelectric intensity
0.1 mV^2
200 ms
Time

Figure 2

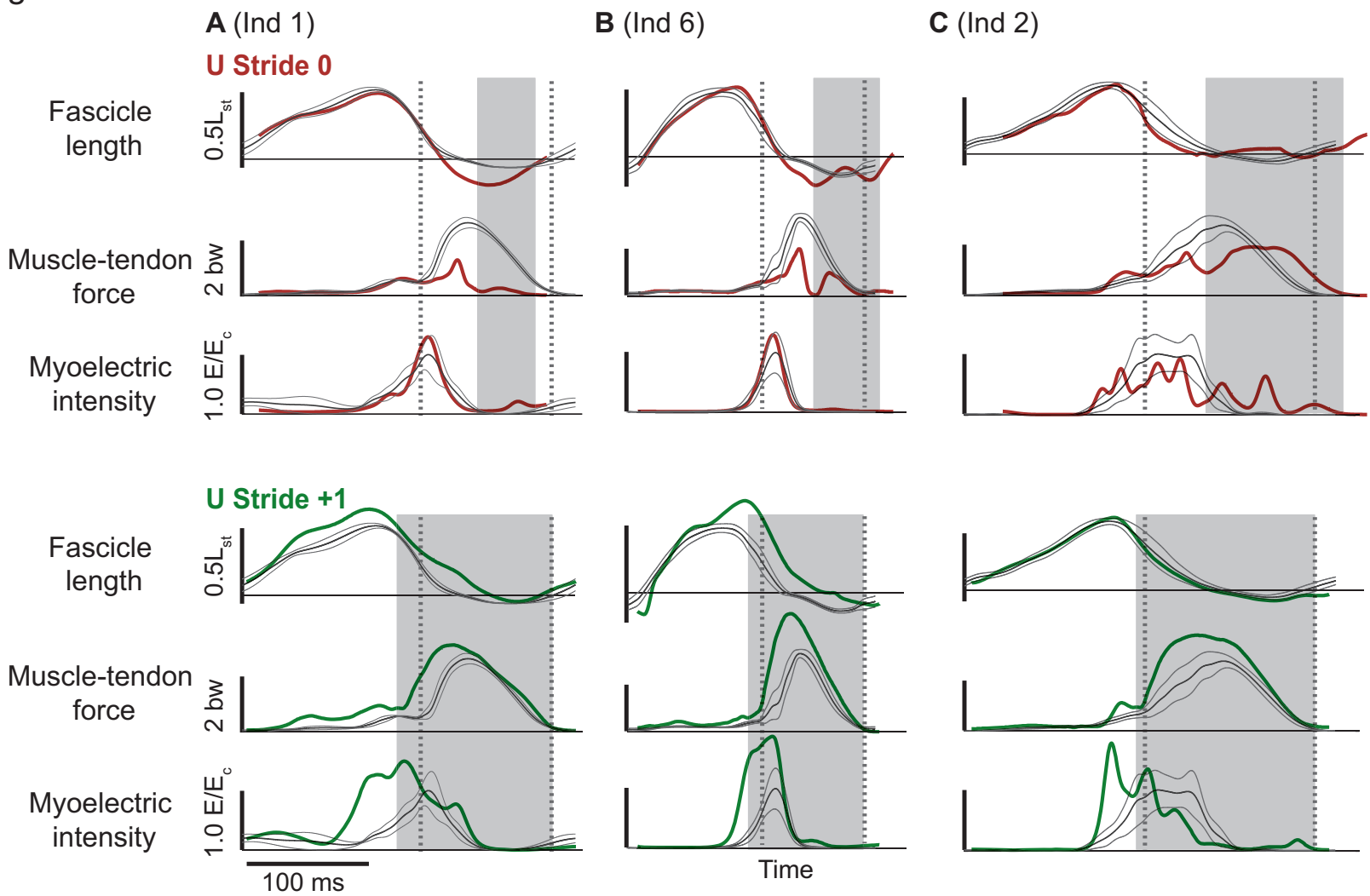
A (Ind 1)
B (Ind 6)
C (Ind 2)
U Stride 0
U Stride +1
Fascicle length
Muscle-tendon force
Myoelectric intensity
0.5L_st
2 bw
1.0 E/E_c
100 ms
Time

Figure 3

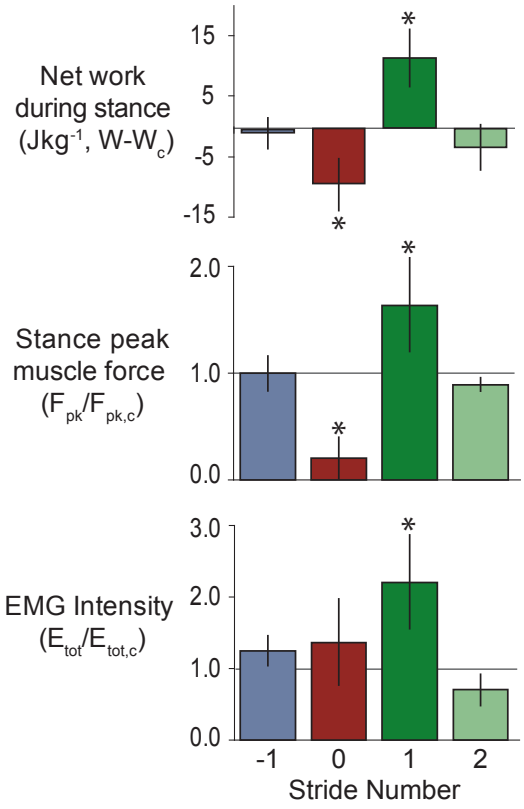
Net work during stance (Jkg-1, W-Wc)
15
5
-5
-15
*
*
Stance peak muscle force (Fpk/Fpk,c)
2.0
1.0
0.0
*
*
EMG Intensity (Etot/Etot,c)
3.0
2.0
1.0
0.0
*
-1
0
1
2
Stride Number

Figure 4

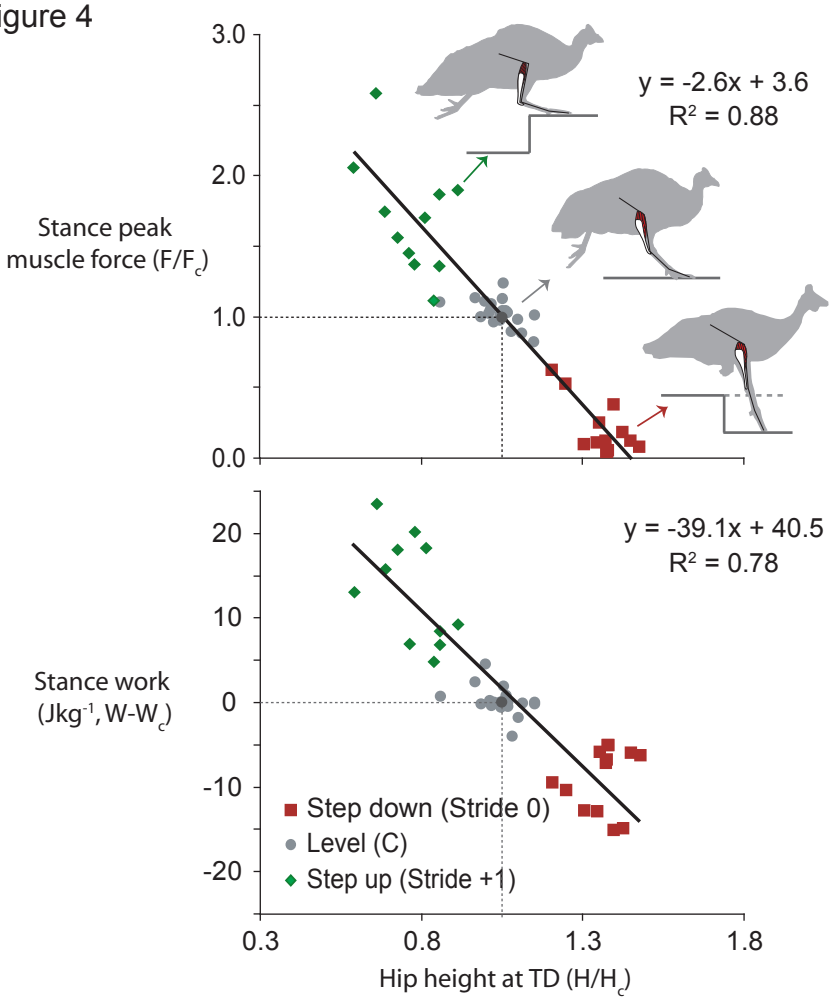
y = -2.6x + 3.6
R² = 0.88
Stance peak muscle force (F/F_c)
3.0
2.0
1.0
0.0
y = -39.1x + 40.5
R² = 0.78
Stance work (Jkg⁻¹, W-W_c)
20
10
0
-10
-20
Step down (Stride 0)
Level (C)
Step up (Stride +1)
0.3
0.8
1.3
1.8
Hip height at TD (H/H_c)